

Supporting Information

Synergistic Toughening of Epoxy Modified by Graphene and Block Copolymer Micelles

Tuoqi Li[†], Siyao He[‡], Andreas Stein[‡], Lorraine F. Francis^{†*}, and Frank S. Bates^{†*}

[†]Department of Chemical Engineering and Materials Sciences, and [‡]Chemistry, University of Minnesota, Minneapolis, MN 55455

RESULTS AND ANALYSIS

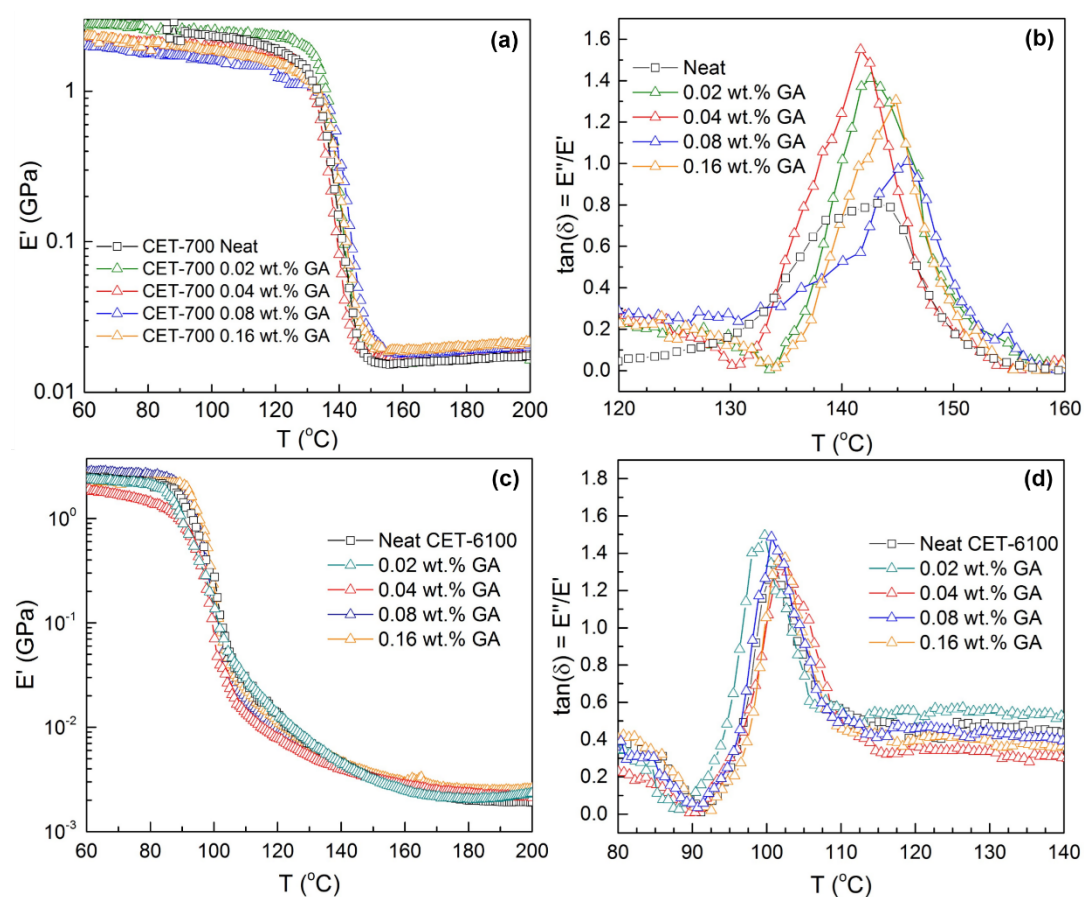


Figure S1. Representative data plots from DMA showing the tensile storage modulus (a, c) and $\tan \delta$ (b, d) as functions of temperature for GA/epoxy binary composites. (a, b) are for the epoxy network with a theoretical $M_c = 700$ g/mol, (c, d) are for the network with theoretical $M_c = 6100$ g/mol.

Table S1. Summary of thermo-mechanical properties, experimental crosslink densities, thermal and mechanical properties of GA/epoxy binary composites.

ID	GA loading (wt.%)	DMA		ρ at 25 °C (g/cm ³)	Experimental M_c (g/mol)	DSC	Elastic
		E_r at 180 °C (MPa)	T_g by max tan δ (°C)			T_g (°C)	modulus at 25 °C (GPa)
CET-700	0	16.8±5.1	143 ± 2	1.203	587 ± 178	141 ± 2	2.75 ± 0.06
	0.02	17.1±1.9	143 ± 1	1.258	603 ± 68	143 ± 3	2.77 ± 0.03
	0.04	17.9±3.9	142 ± 4	1.214	556 ± 122	144 ± 1	2.80 ± 0.08
	0.08	18.9±8.6	146 ± 3	1.293	560 ± 256	141 ± 2	2.90 ± 0.06
	0.16	19.7±4.5	142 ± 2	1.305	543 ± 125	141 ± 2	3.00 ± 0.10
CET-1550	0	8.6±1.9	117 ± 2	1.320	1256 ± 283	115 ± 3	2.68 ± 0.10
	0.04	10.3±4.3	117 ± 3	1.295	1032 ± 432	115 ± 2	2.69 ± 0.08
CET-3050	0	3.4±0.4	105 ± 1	1.189	2849 ± 341	103 ± 2	2.63 ± 0.07
	0.04	3.6±0.8	108 ± 2	1.116	2531 ± 570	105 ± 3	2.70 ± 0.04
CET-6100	0	2.0±0.3	101 ± 2	1.242	5063 ± 740	100 ± 1	2.60 ± 0.05
	0.02	2.1±0.5	100 ± 3	1.253	4886 ± 1100	100 ± 2	2.66 ± 0.07
	0.04	2.2±0.7	102 ± 1	1.307	4957 ± 1558	100 ± 2	2.71 ± 0.06
	0.08	2.3±0.4	101 ± 4	1.328	4711 ± 860	101 ± 1	2.81 ± 0.11
	0.16	2.5±1.1	103 ± 3	1.352	4395 ± 1889	99 ± 3	2.89 ± 0.09

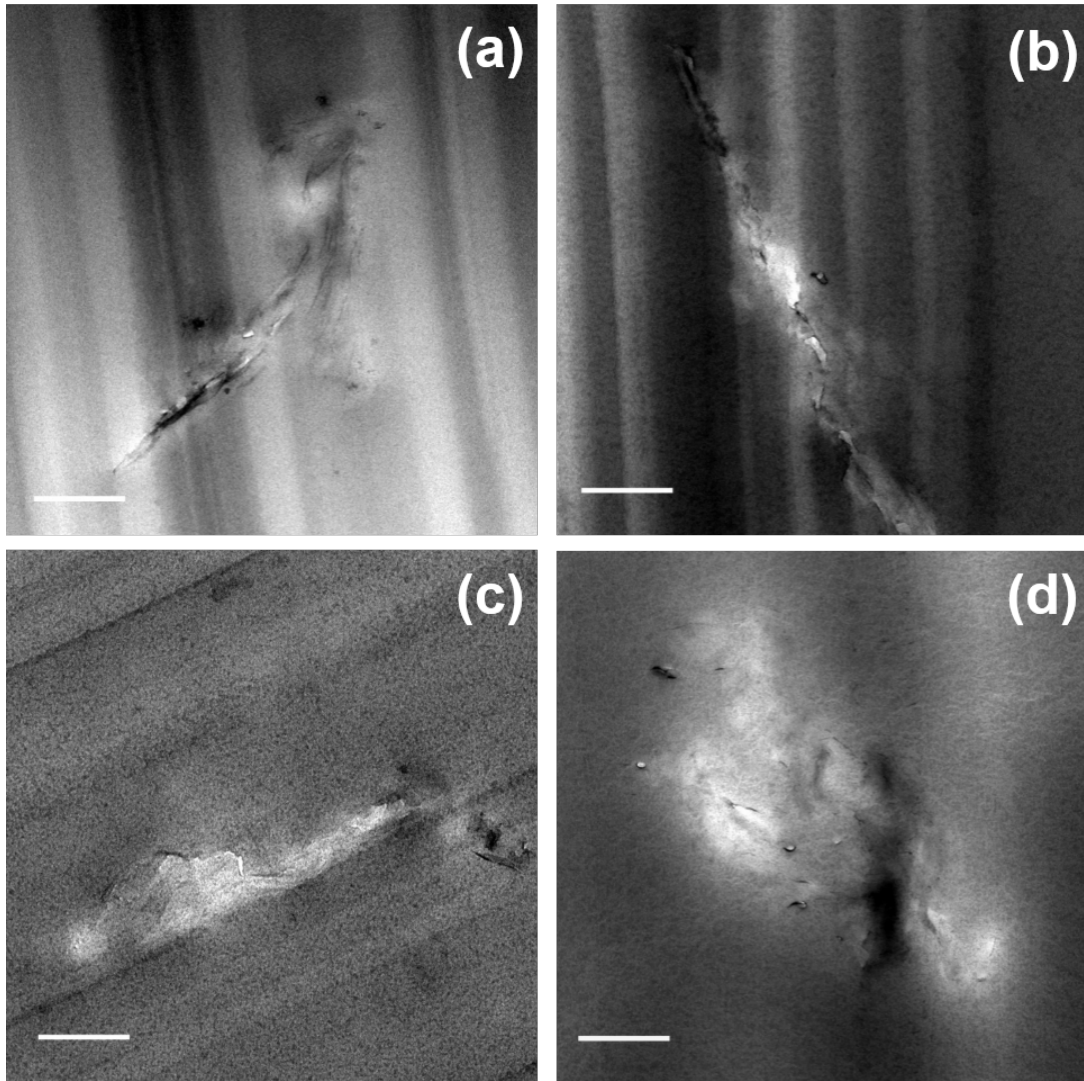


Figure S2. Representative TEM images of cured epoxy/GA binary composites with the theoretical crosslink density (a) $M_c = 700\text{g/mol}$, (b) $M_c = 1550\text{ g/mol}$, (c) $M_c = 3050\text{ g/mol}$, (d) $M_c = 6100\text{ g/mol}$. The loading of GA is 0.04 wt.% in all cases. Scale bars represent 0.5 μm.

Mechanical Properties of GA/epoxy binary composites. In Figure 2a, the room temperature elastic modulus of GA/epoxy binary composites show an approximately linear increase with the loading of GA. Therefore, a modified rule of mixtures has been employed to determine the effective modulus, E_{eff} , of the modifier GA in the CET-700 and CET-6100 systems:^{44, 70}

$$E_c = E_m V_m + E_{eff} V_{GA} \quad (S1)$$

where E_c and E_m are the elastic moduli of the binary composite and epoxy matrix, respectively. V_m and V_{GA} are the volume fractions of the epoxy matrix and the modifier GA, with $V_m + V_{GA} = 1$. Following this relationship, Figure S3a displays the linear regression of the data in Figure 2a, providing that for CET-700, $E_{eff} = 250$ GPa and for CET-6100, $E_{eff} = 303$ GPa. Furthermore, E_{eff} can be related to E_{GA} (the modulus of GA particle) through the relationship $E_{eff} = E_{GA} \eta_0 \eta_1$ where η_0 is the Krenchel orientation factor, which depends on the average orientation of particles within the matrix; η_1 is the length parameter allowing for poor stress transfer at the particle/matrix interface for particles with small lateral dimensions ($\eta_1 = 1$ for perfect stress transfer and $\eta_1 = 0$ for no stress transfer).⁷⁰ There is no observable difference between CET-700 and CET-6100 binary composites in terms of the GA particle orientation within the matrix, according to TEM.

According to Equation (S1), the moduli of 0.04 wt.% GA modified binary composites shown in Figure 2b can be interpreted as the effective modulus of GA as a function of M_c . Figure S3b summarizes the results and displays that E_{eff} increases with

the theoretical M_c . Given the scatter in the data, we cannot make a definitive conclusion about the effect of M_c on the stress transfer at the GA/epoxy interface.

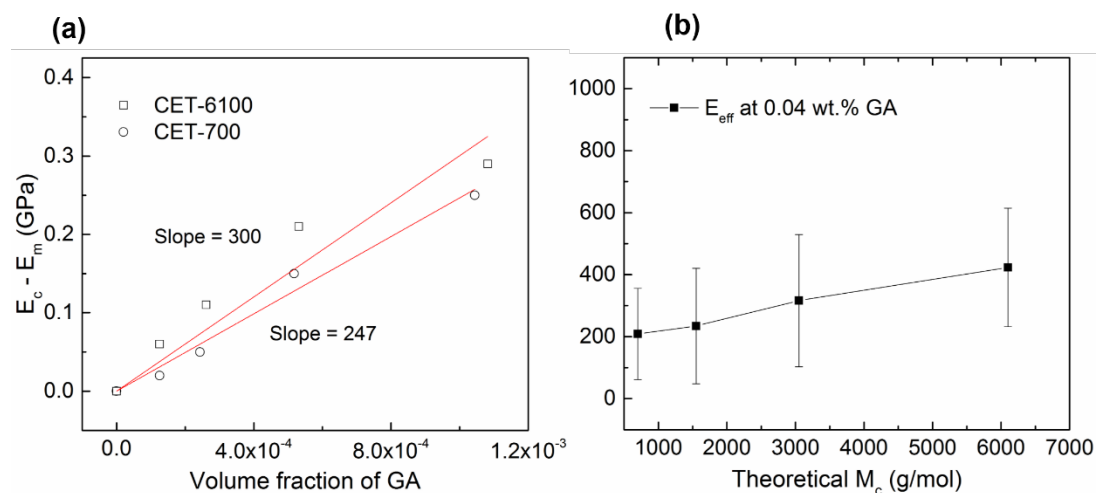


Figure S3. (a) Increment in the elastic modulus ($E_c - E_m$) of GA/epoxy binary composites relative to neat epoxy modulus (E_m) as a function of the GA volume fraction. Linear regressions of the data provide the effective modulus, E_{eff} , of the GA modifier in binary composites, as 250 GPa for CET-700, and 303 GPa for CET-6100, respectively. (b) E_{eff} of binary composites with 0.04 wt.% GA as a function of the matrix crosslink density. All values of E_{eff} were calculated according to equation (S1) based on the data listed in Table S1. The solid line is to guide the eye.

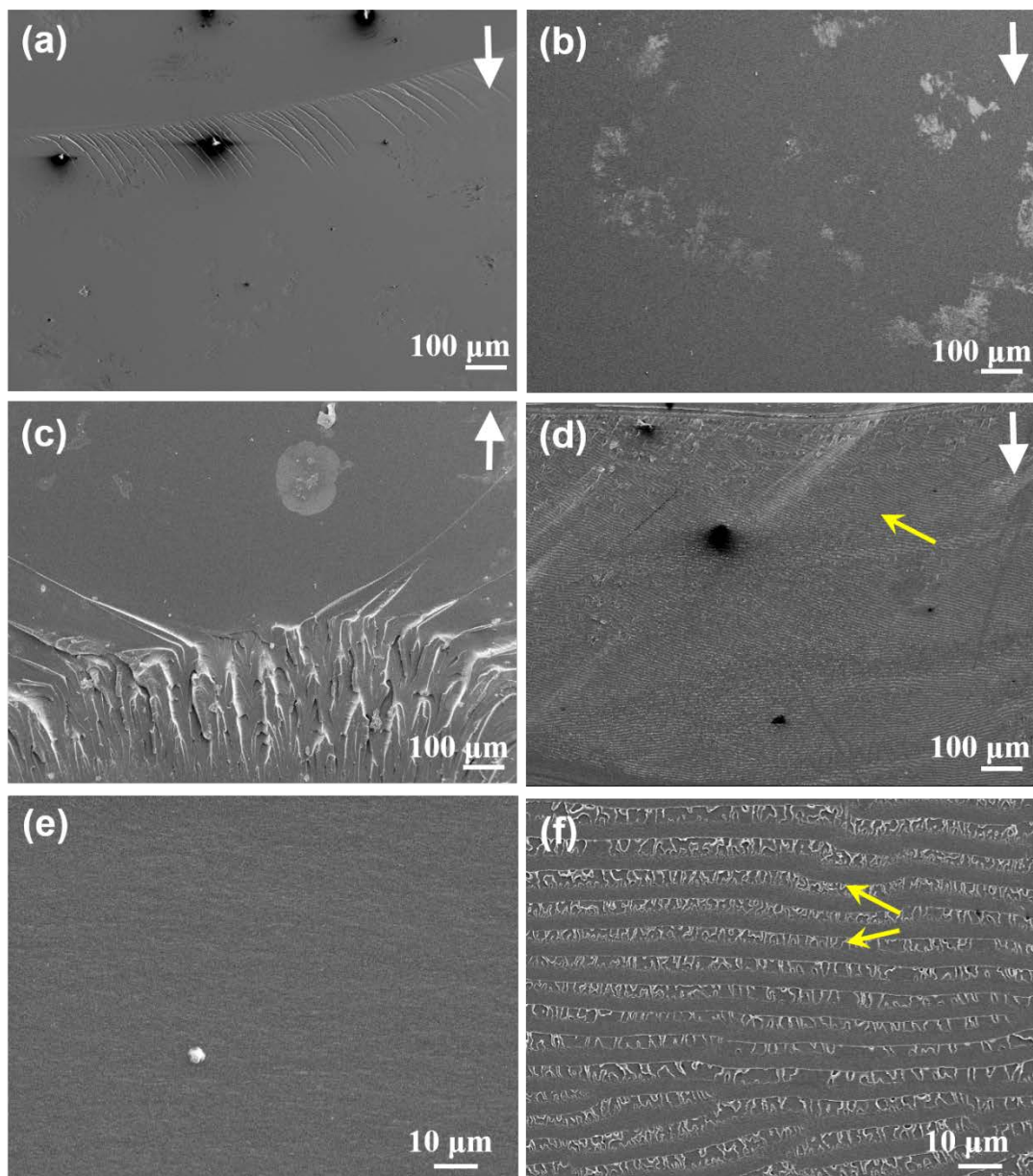


Figure S4. SEM images of the rapid fracture portion of the fracture surfaces of neat epoxies with varying theoretical crosslink densities (a) $M_c = 700$ g/mol, (b) $M_c = 1550$ g/mol, (c) $M_c = 3050$ g/mol, (d) $M_c = 6100$ g/mol. (e) and (f) are the zoomed-in micrographs of images (a) and (d), respectively. White arrows indicate the crack propagation direction. The yellow arrows in (d) and (f) denote the crack-arrest lines in the neat CET-6100 epoxy.

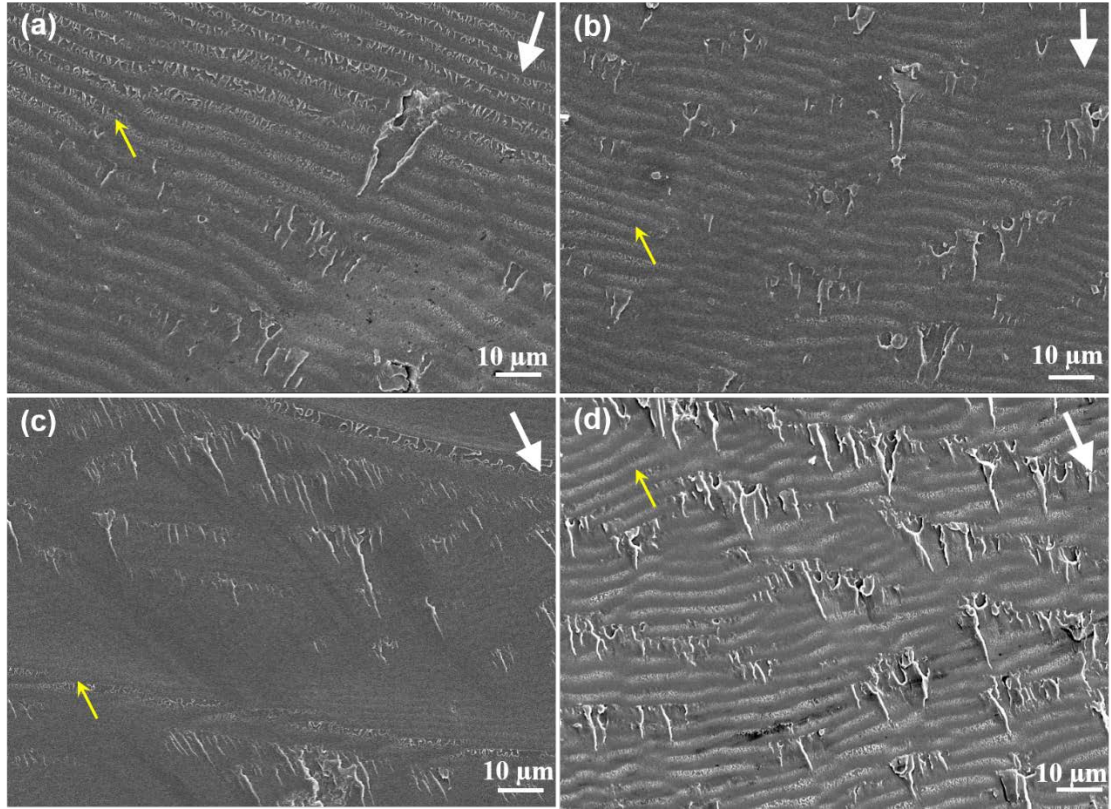


Figure S5. SEM images of the rapid fracture portion of the fracture surfaces of GA/epoxy binary composites with theoretical $M_c = 6100$ g/mol containing different amount of GA (a) 0.02 wt.%, (b) 0.04 wt.%, (c) 0.8 wt.%, and (d) 0.16 wt.%. White arrows indicate the direction of crack propagation and yellow arrows denote the crack-arrest lines.

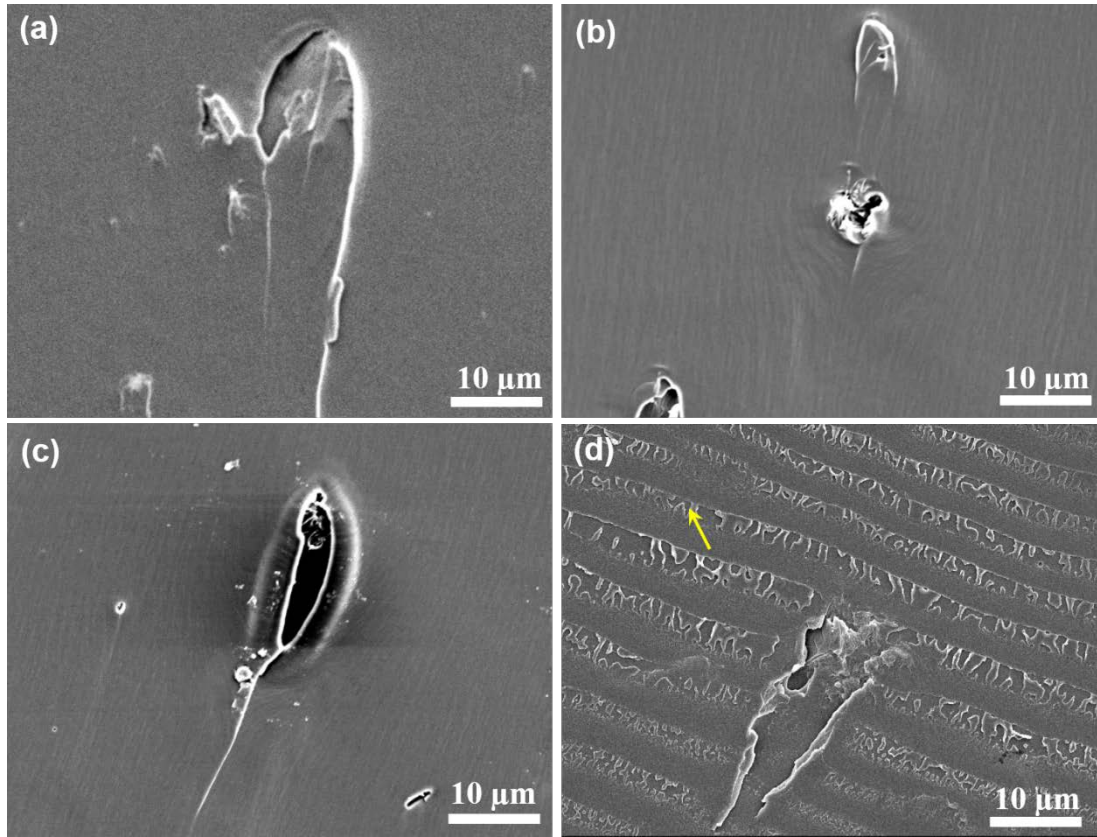


Figure S6. SEM images of the rapid fracture portion of the fracture surfaces of GA/epoxy binary composites with varying matrix crosslink densities (a) CET-700, (b) CET-1050, (c) CET-3050, and (d) CET-6100. The concentration of GA is 0.04 wt.% in all cases. The yellow arrow in (d) indicates the crack-arrest lines.

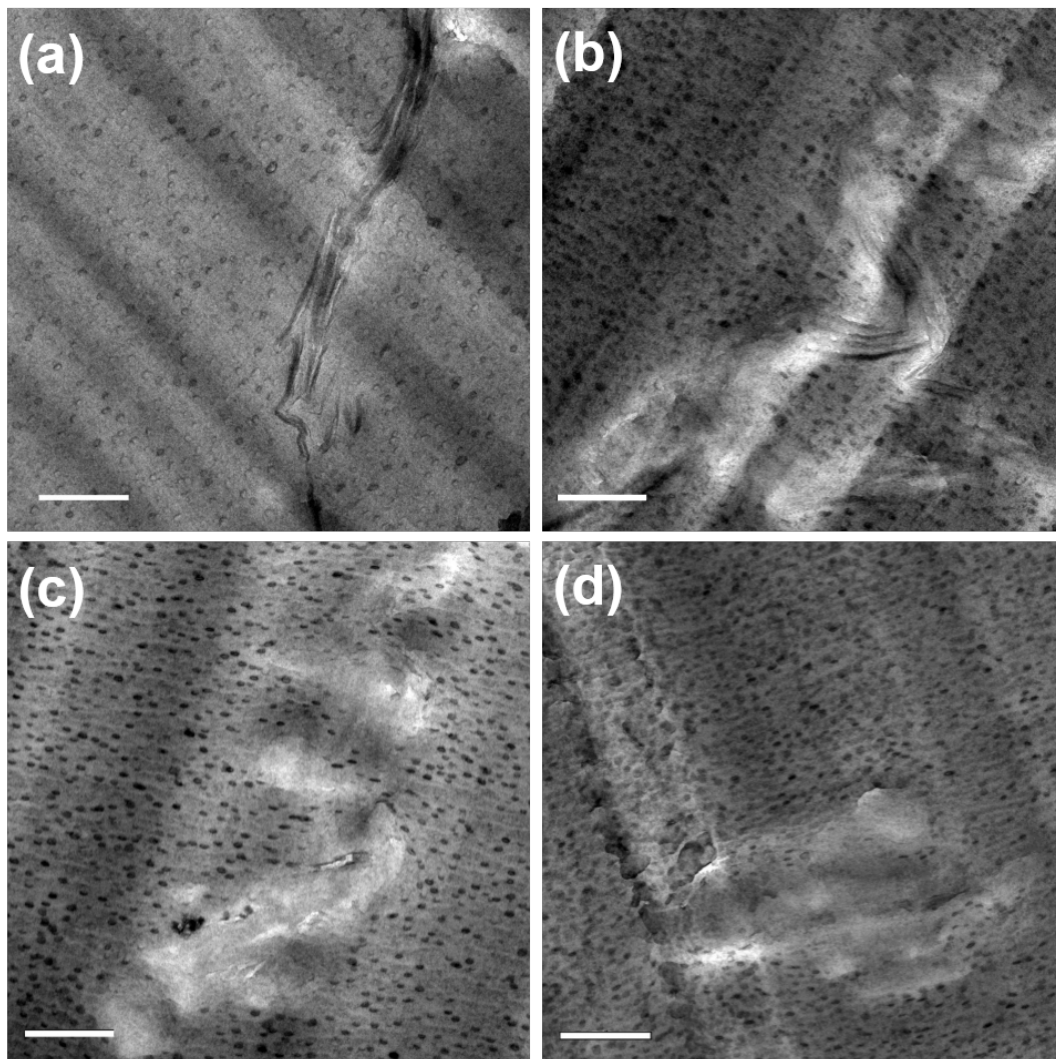


Figure S7. Representative TEM images of cured GA/OP/epoxy ternary composites with the theoretical M_c (a) 700g/mol, (b) 1550 g/mol, (c) 3050 g/mol, (d) 6100 g/mol. The loading of GA is 0.04 wt.% and the loading of OP is 5 wt.% in all cases. RuO_4 , used as a contrast agent, preferentially stains the PEO/epoxy interface, making relatively brighter PEP cores with darker PEO coronas. Scale bars represent 0.5 μm .

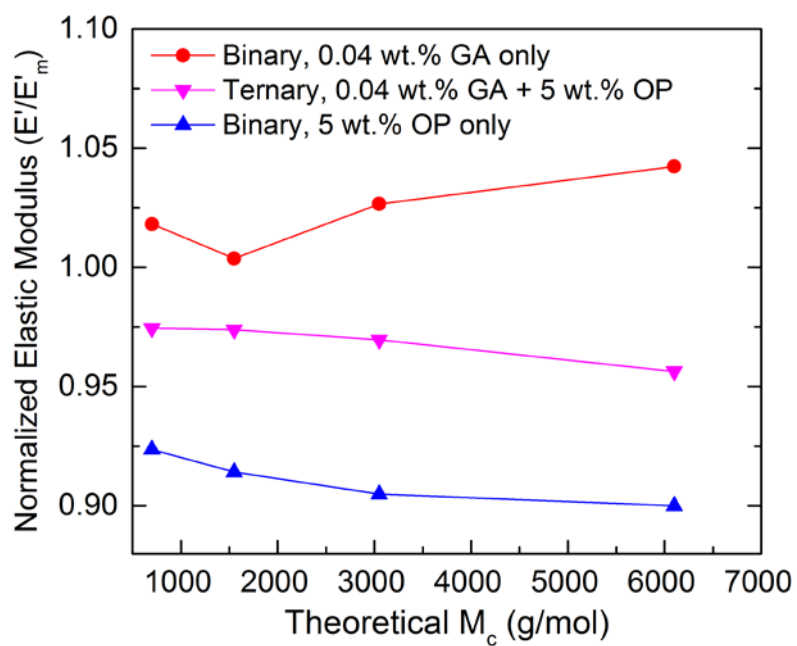


Figure S8. Normalized elastic moduli at 25 °C for cured composites as functions of the theoretical M_c of the epoxy network. For binary composites, the modifier is only 0.04 wt.% GA (,) or only 5 wt.% OP (7). Ternary composites (B) contain both 0.04 wt.% GA and 5 wt.% OP. All normalized values are relative to the moduli of associated neat epoxy resins. Solid lines are to guide the eye.

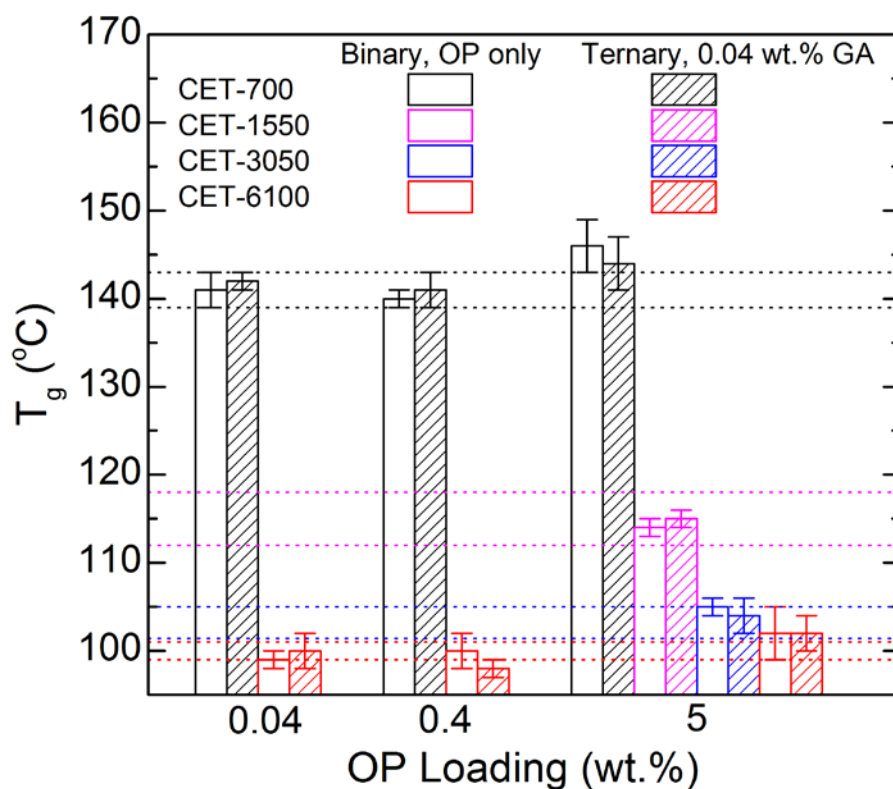


Figure S9. Glass transition temperature (T_g) of the OP/epoxy binary composites and GA/OP/epoxy ternary composites. The loading of GA is 0.04 wt.% in all ternary composites, and the loading of OP varies. The dotted lines in the same color denote the T_g (with experimental uncertainty) of the neat epoxy with associated theoretical M_c value.

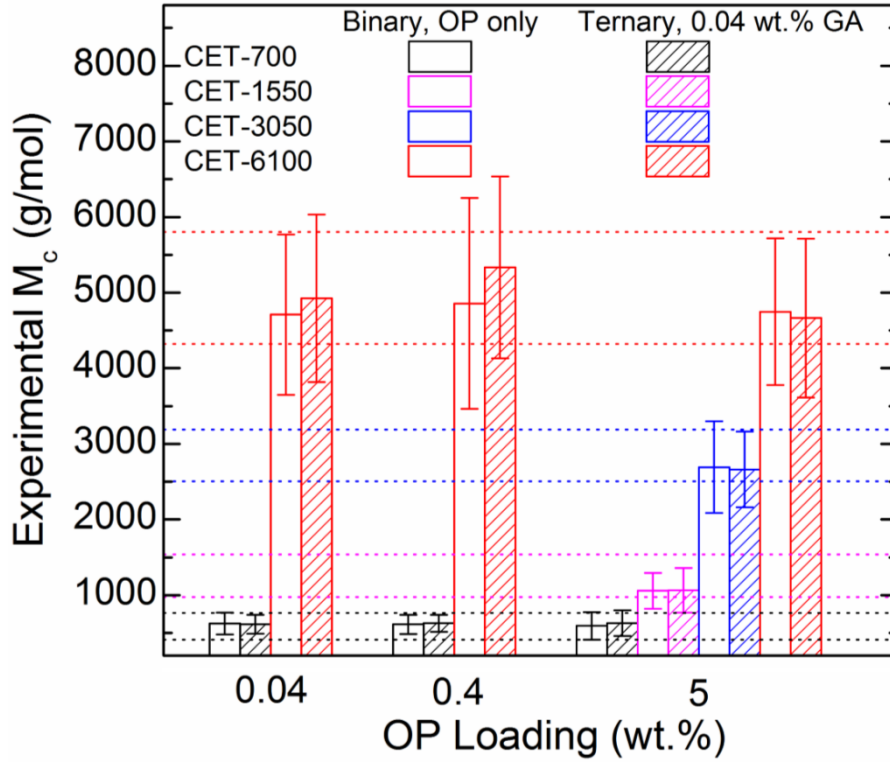


Figure S10. Experimental M_c values of the OP/epoxy binary composites and GA/OP/epoxy ternary composites. The loading of GA is 0.04 wt.% in all ternary composites, and the loading of OP varies. The dotted line in the same color denotes the experimentally measured M_c value (with experimental uncertainty) of the neat epoxy materials.

Table S2. Summary of thermo-mechanical properties, experimental crosslink densities, thermal and mechanical properties of GA/OP/epoxy ternary composites.

Epoxy	Modifier Loading (wt.%)		DMA		ρ at 25 °C (g/cm ³)	Experimental M_c (g/mol)	DSC	Elastic modulus at 25 °C (GPa)
	GA	OP	E_r at 180 °C (MPa)	T_g by max tan δ (°C)			T_g (°C)	
CET-700		0	16.8±5.1	143±2	1.203	587±178	141 ± 2	2.75 ± 0.06
		0.04	15.8±3.7	144±1	1.208	626±145	141 ± 2	2.74 ± 0.09
		0.4	15.7±3.2	141±2	1.176	614±126	140 ± 1	2.69 ± 0.10
		5	15.0±4.6	141±3	1.087	594±181	146 ± 3	2.54 ± 0.09
		0.04	16.6±3.3	144±1	1.251	617±124	142 ± 1	2.75 ± 0.08
	0.04	0.4	15.6±2.8	143±2	1.199	630±112	141 ± 2	2.71 ± 0.05
		5	15.4±4.1	141±2	1.189	632±169	144 ± 3	2.68 ± 0.10
CET-1550		0	8.6±1.9	117±2	1.320	1256±283	115 ± 3	2.68 ± 0.10
		5	9.5±2.1	116±4	1.230	1058±238	114 ± 1	2.45 ± 0.07
	0.04	5	9.7±2.7	116±2	1.260	1064±294	115 ± 1	2.61 ± 0.10
CET-3050		0	3.4±0.4	105±1	1.189	2849±341	103 ± 2	2.63 ± 0.07
		5	3.4±0.8	106±3	1.127	2691±606	105 ± 1	2.38 ± 0.07
	0.04	5	3.7±0.7	105±2	1.187	2663±500	104 ± 2	2.55 ± 0.13
CET-6100		0	2.0±0.3	101±2	1.242	5063±740	100 ± 1	2.60 ± 0.05
		0.04	2.0±0.5	99±1	1.150	4709±1060	99 ± 1	2.58 ± 0.06
		0.4	2.1±0.6	99±1	1.233	4857±1393	100 ± 2	2.55 ± 0.05
		5	2.1±0.4	103±4	1.194	4748±969	102 ± 3	2.34 ± 0.19
		0.04	2.1±0.5	99±2	1.262	4924±1108	100 ± 2	2.59 ± 0.05
	0.04	0.4	1.9±0.4	98±2	1.237	5334±1201	98 ± 1	2.57 ± 0.08
		5	2.1±0.5	101±3	1.207	4664±1050	102 ± 2	2.51 ± 0.10

Table S3. Summary of the K_{Ic} and G_{Ic} of cured ternary composites with different network crosslink densities and modifier loadings.

Sample	Modifier Loading (wt.%)		K_{Ic} (MPa $\cdot\sqrt{m}$)	G_{Ic} (J/m ²)
	GA	OP		
CET-700	0	0	0.86 ± 0.07	238 ± 39
		0.04	1.03 ± 0.10	342 ± 67
		0.4	1.24 ± 0.12	506 ± 100
		5	1.49 ± 0.18	773 ± 189
	0.04	0	0.96 ± 0.08	291 ± 49
		0.04	1.16 ± 0.13	433 ± 98
		0.4	1.43 ± 0.07	667 ± 66
		5	1.65 ± 0.13	898 ± 145
CET-6100	0	0	0.94 ± 0.06	301 ± 39
		0.04	1.10 ± 0.14	415 ± 106
		0.4	1.38 ± 0.07	660 ± 68
		5	3.05 ± 0.18	3516 ± 504
	0.04	0	1.26 ± 0.11	518 ± 91
		0.04	1.33 ± 0.10	604 ± 92
		0.4	1.57 ± 0.13	848 ± 143
		5	3.86 ± 0.40	5250 ± 1108
CET-1550	0	0	0.83 ± 0.07	227 ± 39
		5	2.10 ± 0.12	1592 ± 188
	0.04	0	1.07 ± 0.12	376 ± 85
		5	2.38 ± 0.15	1919 ± 253
CET-3050	0	0	0.91 ± 0.03	278 ± 20
		5	2.75 ± 0.15	2810 ± 318
	0.04	0	1.12 ± 0.08	411 ± 59
		5	3.20 ± 0.31	3551 ± 712

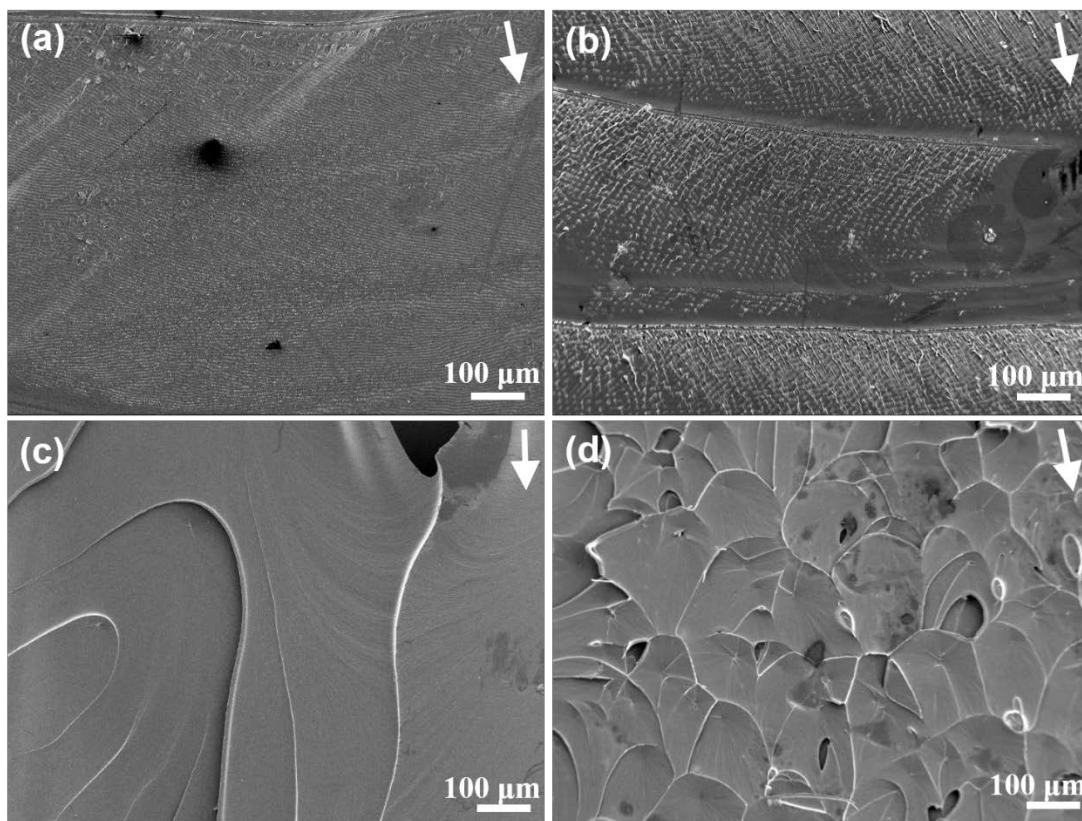


Figure S11. Zoomed-out SEM images of the rapid fracture portion of the fracture surfaces of (a) neat epoxy, (b) GA/epoxy binary composites with 0.04 wt.% GA; (c) OP/epoxy binary composites with 5 wt.% OP; (d) GA/OP/epoxy ternary composites with 0.04 wt.% GA and 5 wt.% OP. The epoxy network has the theoretical $M_c = 6100$ g/mol in all cases. White arrows indicate the crack propagation direction.

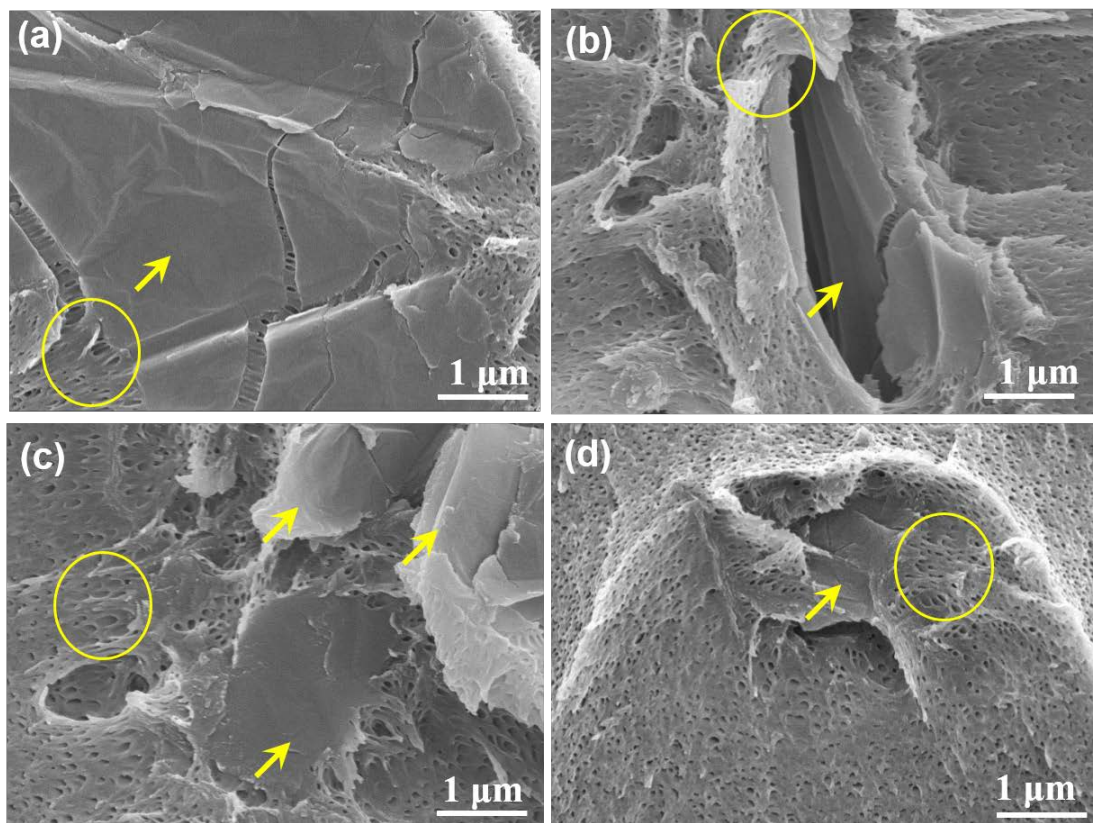


Figure S12. SEM images of the rapid fracture portion of the fracture surfaces of GA/OP/epoxy ternary composites with 0.04 wt.% GA and 5 wt.% OP. The epoxy network is the CET-6100 resin in all cases. The yellow arrows denote the GA particles. The yellow circles in highlight the micelle holes being stretched.

Table S4. Summary of the maximum synergistic toughening effect in epoxy-based ternary composites.

Reference	Modifier type, size and loading		^a ΔK_{Ic}					^b ΔG_{Ic}				
	Rigid additive	Soft additive	Rigid binary	Soft binary	^c Additive toughening	Ternary	Synergy (%) ^d	Rigid binary	Soft binary	^c Additive toughening	Ternary	Synergy (%) ^d
This work	GA, 0.04 wt.%	OP, 5 wt.%	0.34	2.24	2.58	3.11	21%	0.72	10.7	11.4	16.5	45%
47	Silica NP, d ~ 20nm, 14.8 wt.%	CTBN, 9 wt.%	1.19	0.88	2.07	2.71	31%	2.94	3.31	6.25	13.4	114%
50	Silica NP, 20 nm, 5 wt.%	CTBN, 18 wt.%	0.65	1.38	2.03	2.09	3%	--	--	--	--	--
51	Silica sphere, 5 μ m, 30 vol.%	PMMA-PBA diblock copolymer, 5 phr	0.88	0.44	1.32	1.38	5%	--	--	--	--	--
54	Silica NP, 20 nm, 15 wt.%	CTBN, 9 wt.%	0.63	1.84	2.47	2.51	2%	1.48	7.71	9.19	11.5	25%
87	Silica NP, 20 nm, 10 wt.%	CTBN, 10 wt.%	0.52	0.73	1.25	1.28	2%	1.03	2.35	3.38	4.49	33%
56	Interclated organoclay, agglomerates < 1 μ m, 5 wt.%	PPO-PEO diblock, 50-200 nm, 10 wt.%	0.59	0.91	1.50	1.60	7%	--	--	--	--	--

58	Organoclay, agglomerates < 1 μm, 6phr	CTBN, 20 phr	0.72	0.55	1.27	1.14	-10%	1.8	2.75	4.55	6	32%
87	Halloysite clusters < 1 μm, 10 wt.%	CTBN, 10 wt.%	0.49	0.73	1.22	1.28	5%	1.09	2.35	3.44	4.72	37%

^{a,b} ΔK_{Ic} (or ΔG_{Ic}) is defined according to Equation (8). From each reference, only the largest increase in the toughness of the ternary systems has been reported, and the associated modifier loadings are also listed. The toughness values for the binary systems correspond to the composites containing the listed modifier loadings.

^c The additive toughening results are estimated based on Equation (9).

^d The synergy is defined as the relative difference between the ternary results and the additive toughening results. Specifically, the ternary value is divided by the additive toughening value, then the resultant number subtracts one, followed by multiplying 100.

EXPERIMENTAL

Compact Tension Test. A schematic of the compact tension test specimen is presented Figure S13 and the geometry information is specified. Representative load *versus* displacement curves obtained from compact tension tests are shown in Figure S14, where the behavior of the neat and block copolymer modified materials exhibit a linear relationship between load and displacement followed by a catastrophic failure (i.e., rapid crack propagation). ASTM standard D 5045 requires several criteria for verifying the validity of the LEFM approach to determine fracture toughness.

First, in the calculation of K_{Ic} following Equation (2) in the paper, we select the load P_Q following the ASTM procedures. See Figure S15 for an example. Briefly, a best fit line (AB) was draw to the load *vs.* displacement data and a second line (AB') with a compliance (i.e., inverse slope) of 1.05 times that of the original line is drawn. When the maximum load that the specimen was able to sustain, P_{max} , fell within lines (AB) and (AB'), P_Q was taken as P_{max} and used to calculate K_Q . Otherwise, the intersection of line (AB') and the load versus displacement curve, P_Q , was used. Also, when $P_{max}/P_Q < 1.1$, P_Q was used in the calculation of K_Q and if $P_{max}/P_Q > 1.1$, the test was invalid. This restriction limits the magnitude of the ambiguity in the point of crack extension

Second, the following relationship was also used to check the calculated K_Q values:

$$B, a, (W - a) > 2.5 \left(\frac{K_{Ic}}{\sigma_y} \right)^2 \quad (S2)$$

where B is the specimen thickness, a is the crack length and W is the specimen width, and σ_y is the material yield stress determined from a tensile test. This restriction guarantees that the plastic zone size is no more than 2% of the uncracked ligament width, validating plane strain conditions and justifying LEFM analysis.

In this work, we did not measure the yield stress but used literature values to verify the plane strain condition. In the CET epoxy system, take the 0.04 wt.% GA/5 wt.% OP/CET-6100 ternary composite as an example, which exhibits the greatest K_{Ic} value (the range of the data is from 3.45 to 4.0 MPa·√m). According to the reported tensile properties of this CET epoxy thermoset,⁶⁴ the yield stress of neat materials is ~ 77 MPa, independent of the matrix M_c , and σ_y drops to ~ 70 MPa with the addition of 5 wt.% PEO-PEP diblock copolymer. By assuming negligible influence on σ_y from 0.04 wt.% GA (which is supported by the previous work⁴³), so $\sigma_y = 70$ MPa, and $K_{Ic} = 4.0$ MPa·√m, we obtain the right-hand side of Equation (S2) = 8.16 mm. For this specific specimen, B = 8.2 mm, W = 16.5 mm, a = 8.3 mm, the relationship as shown in Equation (S2) still holds. All K_Q values were verified in a similar fashion mm. Therefore, the reported K_Q values in this work can reflect the fracture toughness, K_{Ic} , of the neat and modified thermoset materials.

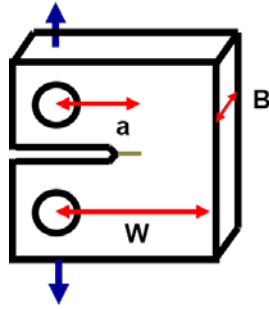


Figure S13. Schematic of compact tension test specimen. Typical dimensions for the specimens are $B = 8.0 \pm 0.3$ mm, $W = 16 \pm 0.5$ mm, and the pre-crack length a (which is the addition of the machined crack length and manually introduced pre-crack length) should fall within $7.2 \text{ mm} < a < 8.8 \text{ mm}$. Likewise, $(W - a)$ therefore is in the range of 7.2 to 8.8 mm.

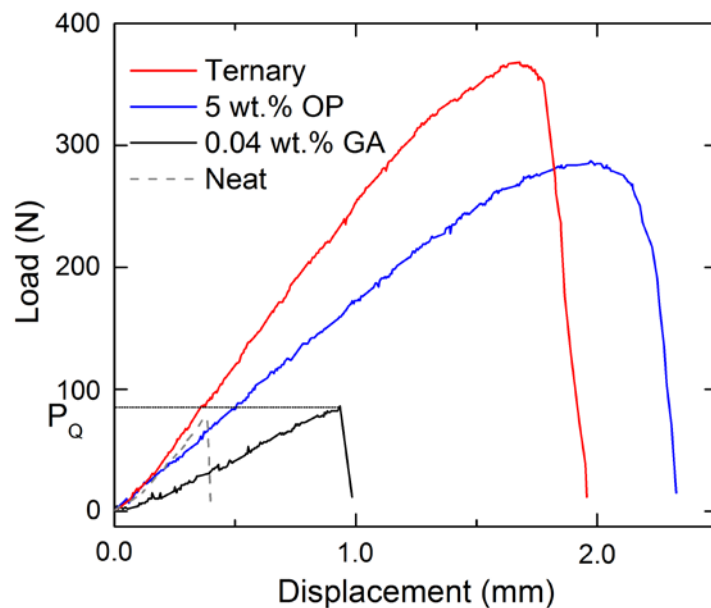


Figure S14. Representative load *versus* displacement curves obtained from compact tension tests. The specimens included here are the CET-6100 neat epoxy (dashed line), the CET-6100/0.04 wt.% GA binary composite (black line), the CET-6100/5 wt.% OP binary composite (blue line) and the CET-6100/0.04 wt.% GA/5 wt.% OP ternary composite (red line). The linear relationship between load and displacement, and the catastrophic failure of the materials justify the use of LEFM for analysis.

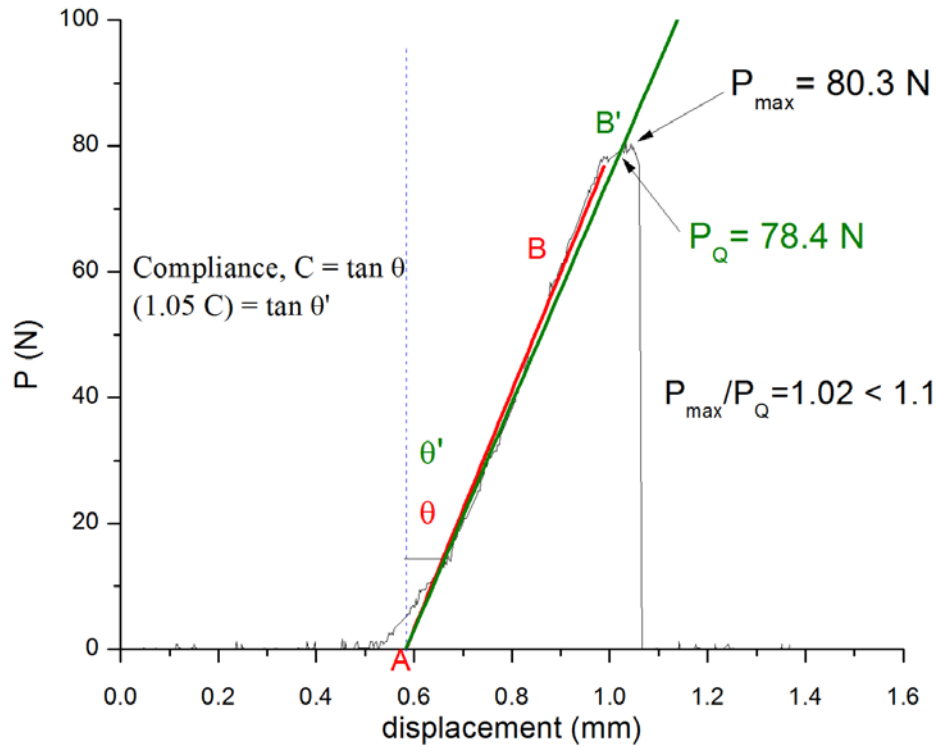


Figure S15. Determination of compliance and force from the load *versus* displacement curve obtained from compact tension tests on representative specimens from the CET-6100/0.04 wt.% GA binary composites. The compliance, C , is the reciprocal of the slope of the linear fitting line AB , and line AB' has a compliance 5% greater than that of line AB . In this example, the maximum load that the specimen can sustain, P_{\max} does not fall with the lines AB and AB' , and $P_{\max}/P_Q < 1.1$, so the test is valid and P_Q should be used in the calculation of K_Q , following Equation (2).